Vol. 558: 35–49, 2016
doi: 10.3354/meps11882

MARINE ECOLOGY PROGRESS SERIES
Mar Ecol Prog Ser

Published October 25

A post-larval stage-based model of hard clam *Mercenaria mercenaria* development in response to multiple stressors: temperature and acidification severity

Cale A. Miller[1,*], George G. Waldbusser[2]

[1]Huxley College of the Environment, Western Washington University, 516 E. College Way, Bellingham, WA 98225, USA
[2]College of Earth, Ocean, and Atmospheric Sciences, Oregon State University, 104 COAS Administration Building, Corvallis, OR 97331, USA

ABSTRACT: Complex biogeochemical processes in the coastal oceans lead to highly variable carbonate chemistry that is further modified by the shifting baseline of pCO_2 caused by ocean acidification. Unfavorable carbonate chemistry, which is pervasive in near-shore, shallow-water deposits, due to high rates of organic matter remineralization and the oxidation of reduced metabolites, has been shown to negatively affect benthic calcifying organisms. For settling infaunal bivalve larvae, such as the hard clam *Mercenaria mercenaria*, pore waters high in CO_2 exert a physiological stress on early post-larval development and homeostasis. The effects of acidification have been shown to increase mortality and reduce calcification for 'just settled' juvenile *M. mercenaria*, a life stage that heavily affects adult clam abundance. To better understand the effects of acidification and temperature on this sensitive life stage, we constructed a post-larval stage-based development model that investigated how varying degrees of aragonite saturation state affect post-settlement survival of juvenile *M. mercenaria*. Initial model simulations predict a similar consistency and trend to field experiments that examined the survival of juvenile *Mya arenaria* residing in buffered and unbuffered sediments. According to our model, the magnitude of acidification had a large effect on post-larval stage duration, which translated to a 60% decrease in total survivors under high variability compared to low variability saturation state scenarios. By modifying temperature-dependent growth rates, we were able to progress juveniles out of the more sensitive life stages faster and, therefore, determined scenarios in which faster growth can reduce exposure to acidification during more sensitive stages.

KEY WORDS: Ocean acidification · Stage-based model · Juvenile clam · *Mercenaria mercenaria* · Temperature-dependent growth · Post-larval development

INTRODUCTION

Anthropogenic fossil fuel emissions have led to the rapid increase of atmospheric CO_2. Its subsequent intrusion into the coastal and global oceans results in ocean acidification (OA), increasing the partial pressure of CO_2 (pCO_2), decreasing carbonate ion (CO_3^{2-}) concentration, and increasing proton concentration (Caldeira & Wickett 2003, Orr et al. 2005). Progression of OA decouples the oceanic carbonate acid-base system via increased buffering of excess protons by carbonate. This exceeds the rate at which the carbonate ion pool replenishes, thereby reducing the aragonite and calcite saturation state ($\Omega_{ar/cal}$) of calcium carbonate ($CaCO_3$) in surface waters by decreasing its thermodynamic stability (Feely et al. 2004, Doney et al. 2009, Hönisch et al. 2012). In near-shore coastal waters where physical and biological processes such as riverine input and production and respiration dominate carbonate chemistry variability, a shifting base-

*Corresponding author: mille454@students.wwu.edu

line of atmospheric CO_2 will result in an increased frequency and magnitude of low saturation state events and, therefore, longer periods of vulnerability for calcifying organisms sensitive to the less favorable carbonate chemistry (Feely et al. 2010, Harris et al. 2013, Hauri et al. 2013, Waldbusser & Salisbury 2014, Hales et al. 2016). While it remains unclear if the effects of OA will permeate into the upper sediment layer of near-shore waters, recent evidence suggests that overlaying water rich in CO_2 can disrupt the pH sediment profile when compared to non-enriched water (Queirós et al. 2015). These conclusions suggest that OA could exacerbate the degree of low saturation state and corrosivity in shallow-water deposits; however, additive effects of OA on the carbonate system are difficult to determine given that shallow-water deposits are modulated via biological activity.

In the upper sediment layers, calcite and aragonite pore-water saturation state is characterized as frequently undersaturated due to high rates of organic matter remineralization via aerobic respiration and by the oxidation of reduced metabolites, all of which vary on seasonal and annual timescales (Green & Aller 1998, 2001). The domination of saturation state by surficial aerobic metabolism, however, is dynamic, and cycles diurnally due to the functional and behavioral processes of the microphytobenthos (restricted by irradiance penetration) and macroinfauna on metabolic gas exchange in the upper sediment layers (Wenzhofer & Glud 2004, Tang & Kristensen 2007). Inorganic and organic sediment composition, microbial photosynthesis and respiration, and benthos heterogeneity, therefore, create a mosaic of spatial-specific regions in the upper millimeters of the sediment that have high CO_2 and low saturation state (Glud 2008, Green et al. 2013, Waldbusser & Salisbury 2014). In these shallow-water deposits, where rates of aerobic respiration are high, saturation state is found to be at a minimum (Aller 1982), and this happens to be at the sediment depths where bivalve larvae, settle and metamorphose (Zwarts & Wanink 1989).

The effects of OA have been shown to decrease the survival, settlement, and metamorphosis of developing bivalves, from the larval pediveliger to early juvenile stage classes (Green et al. 2009, 2013, Talmage & Gobler 2009). Post-larval, settling marine bivalves already exhibit significantly high mortality rates (>98%), with ≥30% of the mortality potentially occurring 1 to 2 d after settlement (Roegner & Mann 1995, Gosselin & Qian 1997, Hunt & Scheibling 1997). Multiple modes of mortality have been documented for post-larval juvenile bivalves, with predation being noted as most significant (Thorson 1966, Ólafsson et al. 1994, Gosselin & Qian 1997,). Green et al. (2004, 2009), however, proposed that the geochemical undersaturation of aragonite may be a significant contributor, as they identified that 'just settled' juvenile hard shell clam *Mercenaria mercenaria* experienced higher rates of mortality when exposed to undersaturated conditions, relative to supersaturated. While physical shell dissolution was observed, the exact mechanism inducing mortality was not identified. In a related study on *M. mercenaria*, Waldbusser et al. (2010) determined that juvenile calcification rate decreased with saturation state, and that the effects of low saturation were more pronounced at smaller post-larval stages, precluding net positive calcification for the smaller size classes (i.e. calcification by larger clams was less sensitive to undersaturation). Since a proportional relationship exists between calcium carbonate saturation state and the substrate-to-inhibitor ratio (SIR) — i.e. $[HCO_3^-/H^+]$ — through the thermodynamic equations, the relative significance of either to calcification is still under examination (Thomsen et al. 2015, Waldbusser et al. 2015b).

The metamorphosis of *M. mercenaria* follows larval pediveliger settlement to the benthos, where complete reorganization of the larval body plan occurs, involving adult organ growth (e.g. kidneys and heart), development of the mantle and siphons, and production of the dissoconch I shell (Carriker 2001). During metamorphosis, hard clams are unable to feed for ~2 d, and are wholly reliant upon endogenous energy stores from their larval stage (Carriker 2001 and references therein). The energetic demand of metamorphosis, therefore, places a natural physiological constraint on post-larval juveniles, and increases susceptibility to abiotic stressors, such as acidification (García-Esquivel et al. 2001, Waldbusser et al. 2010). The kinetic constraint and high energetic demand imposed by rapid biocalcification in undersaturated waters with limited energy has been noted for larval bivalves (Waldbusser et al. 2013, 2015a). Thus, shifts in energy allocation toward protein turnover and ion transport increase as a means to maintain physiological homeostasis under OA stress for larval calcifiers (Pan et al. 2015). If the effects of acidification reduce the amount of available ATP invested toward protein-specific synthesis of the energetically costly organic matrix, which is the nucleation site for calcium carbonate precipitation (Lowenstam 1981, Palmer 1992, McConnaughey & Gillikin 2008, Melzner et al. 2011, Waldbusser et al. 2013), then the reduction in calcification recorded by post-larval *M. mercenaria* (Waldbusser et al. 2010) at

undersaturation may be attributable to the stringent energy budget during the period of metamorphosis, and growth stages directly after.

The development of feeding siphons and calcification organs following metamorphosis is commensurate to juvenile hard clam size, and determines feeding efficiency (Carriker 2001, Grizzle et al. 2001 and references therein). The decreased sensitivity to the effects of acidification at larger post-larval sizes (Green et al. 2009, Waldbusser et al. 2010) therefore implies that larger juvenile clams can acquire energy faster, rebuild a depleted energy budget, and build shell more effectively, thus coping with less favorable seawater chemistry. In order for *M. mercenaria* to transition quickly past this physiological bottleneck, pediveligers must successfully settle onto often corrosive sediments, maintain physiological homeostasis, and develop at an undeterred rate to the early juvenile stage. The sensitivity of *M. mercenaria* pediveligers and early juveniles to acidification delineates a specific vulnerable period during development that can heavily affect the adult segment of the population, and may become increasingly important as OA and eutrophication potentially exacerbate less favorable carbonate chemistry conditions within coastal marine sediments.

To integrate experimental data on the acute response of pediveliger and byssal plantigrade (early juveniles) hard clams to changes in carbonate chemistry, we constructed a post-larval stage-based development model of a cohort before, during, and immediately following metamorphosis under multiple degrees of acidification severity, which is described as the product of the intensity and duration of a low saturation state event (Sheffield & Wood 2008, Hauri et al. 2013). Among the myriad processes affecting mortality during this crucial life stage (e.g. predation and bacterial infection), we focused specifically on the effects of aragonite saturation state (Ω_{ar}, hereafter 'saturation state') on growth and survival, and examined how temperature increase may be able to offset slow growth induced by undersaturation of post-larval *M. mercenaria*. Given that little to no field data currently exist on the success of settled juveniles <1 mm shell length (Fegley 2001), we utilized several laboratory studies to parameterize the model. To validate our model, we compared model predictions to experimental results from Green et al. (2013). Specifically, our objectives were to (1) identify how undersaturation affects growth to a larger 'escape' size class, (2) compare proportional differences in final 2.0 mm clam abundances under deterministic and stochastic saturation state as well as variation in settlement patterns, and (3) assess whether temperature-dependent growth rates can overcome effects of acidification on late larval and early juvenile clams.

MATERIALS AND METHODS

Matrix model

We constructed a 7-stage projection matrix model (Lefkovitch 1965) to predict the effects of saturation state dependent survival and growth (calcification) of pediveliger and byssal plantigrade hard shell clams with the MathWorks software Matlab (V. R2013a, b). The model begins 10 d post fertilization when larval clams are in the pediveliger stage, determinate by a swimming-crawling lifestyle and prodissoconch II shell (Carriker 1961). This initial stage class is followed by 6 sequential stages of post-metamorphosis development by the juvenile byssal plantigrade. Stages were based on sizes of 0.2, 0.4, 0.6, 0.8, 1.0, and 2.0 mm (denoted as important by Carriker 2001, Chapter 3), where the 0.2 mm juvenile stage is the newly metamorphosed benthic byssal plantigrade (Fig. 1). The model utilizes an hourly time step for a total duration of 60 d (1440 h). We assigned the 2.0 mm stage class as the endpoint for the model because it has been deemed an 'escape size' from moderate acidification effects on survival and growth in lab based studies (Green et al. 2009, Waldbusser et al. 2010). All surviving juveniles at the final time point (t_f) are considered to successfully join the adult segment of the population, with the explicit caveat that all other growth and mortality factors such as food supply, egg lipid content, predation, and salinity are not considered in this model.

Model parameters

Vital rates for the model, survival, intrinsic growth (height of shell), and stage duration were determined from laboratory and field experiments published in the primary literature, as outlined below. We used multiple linear regression analyses with time and saturation state as independent variables to calculate hourly survival rates for the pediveliger and byssal plantigrade stages based on laboratory experiments from Talmage & Gobler (2009) and Green et al. (2009). Both studies utilized 3 discrete treatments of low, medium, and high saturation states, which were used to construct the linear trend for survival; minimum saturation state values were ~0.8 and 0.4 for

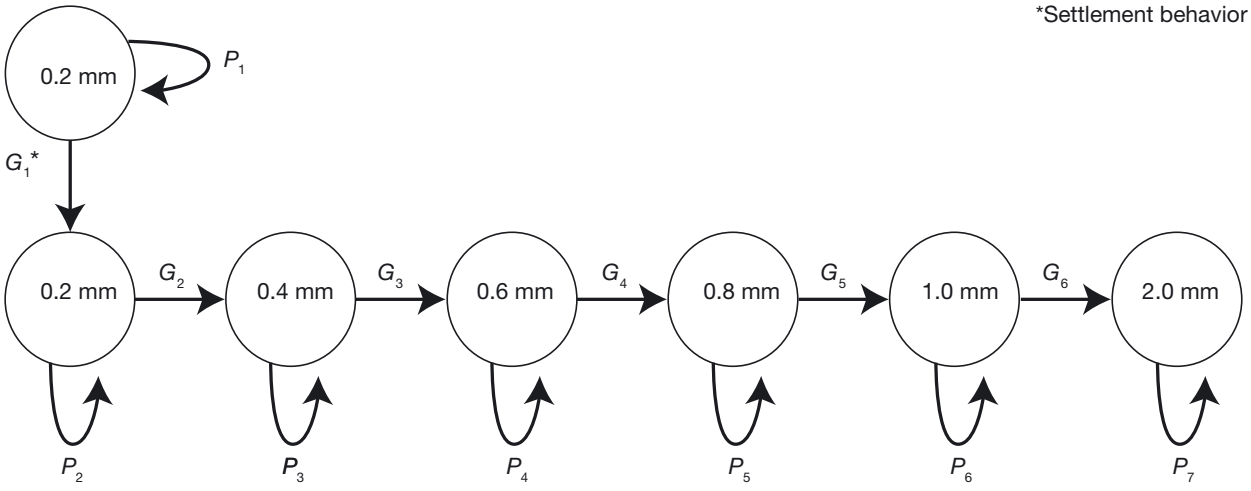

Fig. 1. Conceptual diagram of a 7-class, stage-based, matrix model of hard clam *Mercenaria mercenaria* development from larval pediveliger (0.2 mm shell height) to juvenile byssal plantigrade (2.0 mm). Projection parameter $P_{i,}$ is the probability of surviving and staying in a given stage (retention); G_i is the probability of growing to the next stage (transition). All G_i values are a function of growth (i.e. calcification), with the exception of G_1, which is derived from settlement behavior

Talmage & Gobler (2009) and Green et al. (2009), respectively. Survival rates were extrapolated when necessary from the multiple linear regressions. Due to the lack of empirical data for juveniles <1 mm, we used intrinsic growth rates from the larval period for all juvenile stages. We calculated this to be 8.8% d^{-1}, which was determined from culture experiments examining size of larvae at settlement as a function of temperature (Loosanoff 1959). Multiple field studies from Ansell (1968) determined that optimal growth temperature follows a Gaussian distribution that peaks at 24°C; therefore, we utilized the growth rate from Loosanoff (1959) corresponding to 24°C, i.e. 8.8% d^{-1}. The per degree decrease in growth rate outside of the optimal temperature range was determined by fitting a non-linear curve to the percent decrease in growth of larval clams at 24 and 28°C, as examined by Talmage & Gobler (2011). We derived the saturation state dependent stage duration for byssal plantigrades as:

$$d_i = \left(\frac{\log \frac{SH_{i+1}}{SH_i}}{m} - \sum_{i=2}^{5} d_{i-1} \right) \cdot (2 - gom) \quad (1)$$

where d_i is the stage duration at an ith stage class (i.e. 0.2, 0.4, 0.6, 0.8, or 1.0 mm juvenile sizes), and SH is the shell height at a given stage. The intrinsic growth rate, m, is expressed as % h^{-1}, calculated from 8.8% d^{-1}. This rate is temperature-dependent, however, and was recalculated as described above when simulations incorporated temperature effects. The *gom* term is the proportion by which saturation state affects growth, and is based on the non-linear relationship of calcification (a proxy for growth rate) as a function of saturation state, as examined by Waldbusser et al. (2010). Based on these findings, we fit a 4-parameter Gompertz function to describe the response of growth rate to saturation state, in which the effect of saturation state on growth produced an output proportional term, *gom*. It should be noted that stage duration for the first stage class of pediveliger (d_1) was not calculated using the above equation. This is because pediveligers metamorphose rather than increase shell height when transitioning to byssal plantigrades. Rather, the d_1 parameter was calculated from a logistic regression model applied by Green et al. (2013) to fit experimental laboratory data examining pediveliger acceptance or rejection of undersaturated substrate; thus, the probability of settlement was applied to the d_1 parameter.

Vital rates were then used to construct and calculate the model parameters — probability of survival and retention within a stage (P_i) and probability of transition to the next stage (G_i) — as:

$$P_i = S_i \cdot \left(\frac{1 - S_i^{(d_i - 1)}}{1 - S_i^{d_i}} \right) \quad (2)$$

and

$$G_i = \left(\frac{S_i^{d_i} \left(1 - S_i\right)}{1 - S_i^{d_i}} \right) \quad (3)$$

where S_i is the stage-specific survival probability and d_i the stage-specific duration (Crouse et al. 1987). The parameters (i.e. projection parameters, Table 1) where then input into a projection matrix that collated the probabilities for all stage classes to be modeled in the *SR* 1 model:

Table 1. Projection matrix for life stage development of hard clam *Mercenaria mercenaria* showing parameter values for all stage classes at the initial time point only (probabilities vary by the hour). Ω_{ar}: aragonite saturation state; Ped: pediveliger; Juv: juvenile; *P*: probability of survival and retention within a stage; *G*: probability of transition to the next stage. The projection matrix shows values of *G* and *P* (in that order across the rows) calculated on the basis of an intrinsic growth rate of 8.8% d^{-1} at 24°C. Vertical lines in Columns 1 and 2 indicate identical values from top to bottom

Ω_{ar}	Time point	Stage class	Projection parameter	Projection matrix						
1.2	$t-1$	0.2 mm Ped	P_1	0.0278	0	0	0	0	0	0
|	|	0.2 mm Juv	G_1, P_2	0.9521	0.9928	0	0	0	0	0
|	|	0.4 mm Juv	G_2, P_3	0	0.0033	0.9902	0	0	0	0
|	|	0.6 mm Juv	G_3, P_4	0	0	0.0077	0.9875	0	0	0
|	|	0.8 mm Juv	G_4, P_5	0	0	0	0.012	0.984	0	0
|	|	1.0 mm Juv	G_5, P_6	0	0	0	0	0.0155	0.9948	0
1.2	$t-1$	2.0 mm Juv	G_6, P_7	0	0	0	0	0	0.0049	1

$$\begin{bmatrix} ST_1 \\ ST_2 \\ ST_3 \\ ST_4 \\ ST_5 \\ ST_6 \\ ST_7 \end{bmatrix}_t = \begin{bmatrix} P_1 & 0 & 0 & 0 & 0 & 0 & 0 \\ G_1 & P_2 & 0 & 0 & 0 & 0 & 0 \\ 0 & G_2 & P_3 & 0 & 0 & 0 & 0 \\ 0 & 0 & G_3 & P_4 & 0 & 0 & 0 \\ 0 & 0 & 0 & G_4 & P_5 & 0 & 0 \\ 0 & 0 & 0 & 0 & G_5 & P_6 & 0 \\ 0 & 0 & 0 & 0 & 0 & G_6 & P_7 \end{bmatrix} \cdot \begin{bmatrix} ST_1 \\ ST_2 \\ ST_3 \\ ST_4 \\ ST_5 \\ ST_6 \\ ST_7 \end{bmatrix}_{t-1}$$

where the resultant left cohort vector at time *t* is the product of the projection matrix and the right cohort vector at time $t-1$, and *ST* is the number of individuals in a given stage class.

Model simulations and saturation state variability

To validate the model, simulations were run at constant saturation state values 1.4 and 0.6 under a pulsed settlement scenario (*SR* 1 model), which were used to replicate and compare against the experimental field data (Fig. 2) from Green et al. (2013); where crushed shells were used to buffer sediment plots in a sheltered intertidal mudflat in Portland Harbor, ME. Adjacent buffered and unbuffered plots were compared to determine the response of clam settlement to sediment saturation state. In order to make results comparable, we rescaled our model projections (of 100 individuals) and the Green et al. (2013) data to a maximum density counted, as we did not have larval abundance from the field experiments. It is important to note that the Green et al. (2013) experiments where performed with soft shell clam *Mya arenaria* rather than *Mercenaria mercenaria*, and that the field data does not provide specifics on size distribution; however, the settlement pulse in those cold waters is very abrupt. All subsequent simulations run after the initial model comparison to Green et al. (2013) had a starting cohort size of 360 pediveligers over a 1 m^2 area, which was based on density distributions identified by Carriker (1961) in a cubed meter of water from summer *in situ* sampling in Little Egg harbor, NJ characterized by high uniform salinity, dense aggregations of *M. mercenaria* adults, and a negligible flushing rate. The following simulations examined the effect of saturation state on stage duration. The constant saturation state values for those simulations are the maximum and minimum values of each variability scenario (Fig. 3).

The degrees of saturation state variability for model simulations are intended to represent the diurnal variability of biogeochemical processes occurring in the upper sediment layer. Since there is limited

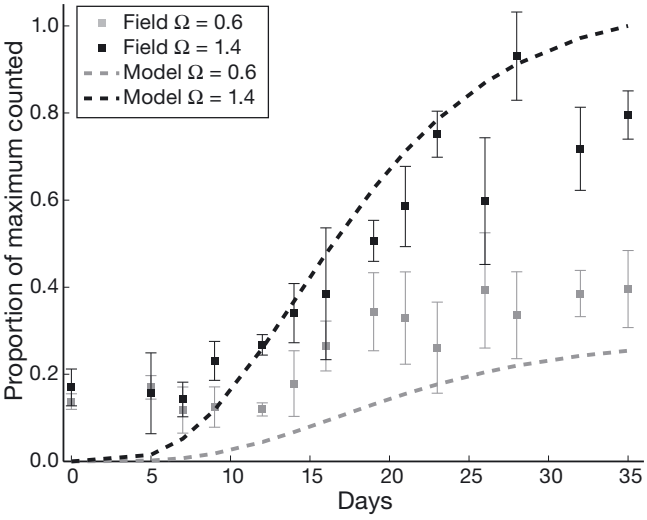

Fig. 2. Comparison of model predictions and field data for hard clam *Mercenaria mercenaria*: proportion of pediveligers counted in field experiments (Green et al. 2013) from settlement to 35 d post settlement in control (■) and buffered (■) sediment pore water, and corresponding model predictions for controlled (dashed gray line) and buffered (dashed black line) sediment pore water. Error bars are SD

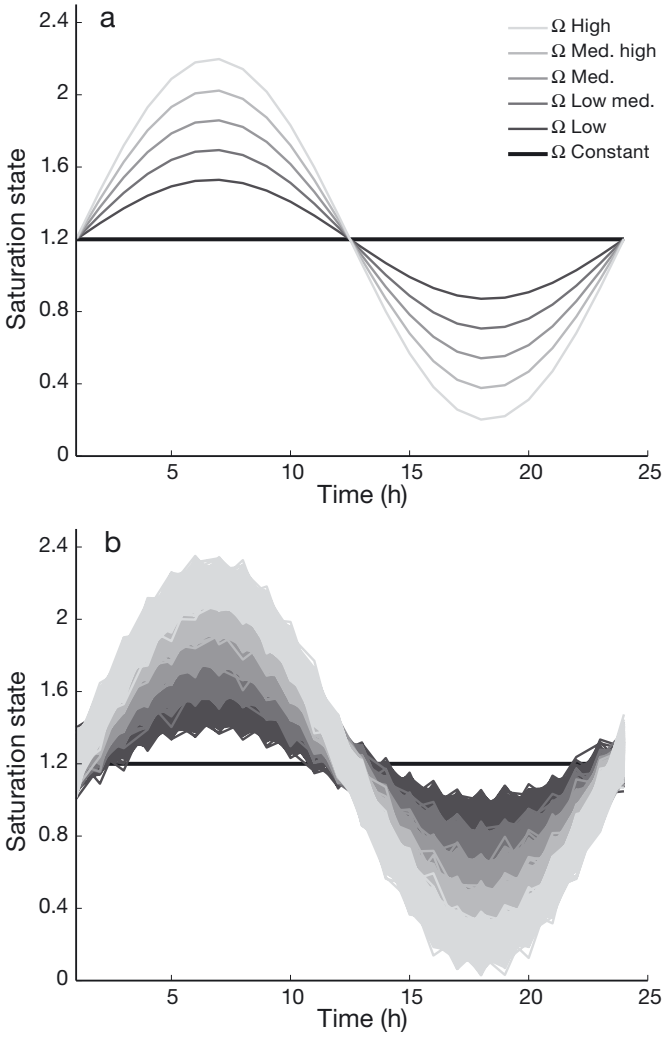

Fig. 3. Five degrees of aragonite saturation state (Ω_{ar}) variability over a 24 h period: low (±0.33), low medium (±0.495), medium (±0.66), medium high (±0.825) and high (±1.0), with a mean Ω_{ar} = 1.2 for all scenarios. (a) Each saturation state variability scenario without stochasticity. (b) 1000 iterations of each saturation state variability scenario with stochasticity

data quantifying the diurnal changes in sediment saturation state, approximations were based on limited studies and we used our discretion when deciding an acceptable range of reported discrete high and low values (Green & Aller 1998, Tang & Kristensen 2007, Green et al. 2013). Five sinusoidal functions with a mean saturation state of 1.2 and amplitudes ranging 33.0, 49.5, 66.0, 82.5, and 100% of a full Ω_{ar} unit over a 24-h period were chosen as the different variability scenarios for the model, which was formulated using the generic function:

$$f(t) = a \cdot \sin \frac{b}{2\pi} + c \quad (4)$$

where a is the amplitude (% of 1 Ω unit), b is the time vector (24 h), and c is the vertical shift (Ω_{ar} = 1.2) (Fig. 3). We chose to include this variability component as it helps approximate change in vital rates by inducing hourly changes in the retention (P_i) and transition (G_i) projection parameters by fluctuating the saturation state (changing the '*gom*' term). That is, as saturation state shifts lower it will reduce the stage duration and survival rate; therefore, higher variability (i.e. increasing the magnitude of low saturation state) will result in a reduced number of post-larval juveniles because their abundance is simply a product of the projection matrix and cohort vector at any given time (see *SR* 1). To introduce environmental and organismal stochasticity to each variability scenario, a Gaussian distribution of white noise was applied using a built-in Matlab function and setting the signal-to-noise ratio at 25. This resulted in an average integrated percent variance of 7.3% for all scenarios over 1000 simulations (Fig. 3b). The 5 different amplitudes for each scenario represent low, low medium, medium, medium high, and high saturation state variability (mean saturation state, Ω_{ar} = 1.2).

Settlement behavior

In addition to the 5 variability scenarios, 2 different settlement regimes were assessed in the model: pulsed and diffused. While nearly all model simulations were run using the pulsed settlement regime, which followed the *SR* 1 model, a diffused settlement regime was applied to a handful of simulations. The diffused settlement regime followed the *SR* 2 model:

$$\begin{bmatrix} ST_1 \\ ST_2 \\ ST_3 \\ ST_4 \\ ST_5 \\ ST_6 \\ ST_7 \end{bmatrix}_t = \left(\begin{bmatrix} P_1 & 0 & 0 & 0 & 0 & 0 & 0 \\ G_1 & P_2 & 0 & 0 & 0 & 0 & 0 \\ 0 & G_2 & P_3 & 0 & 0 & 0 & 0 \\ 0 & 0 & G_3 & P_4 & 0 & 0 & 0 \\ 0 & 0 & 0 & G_4 & P_5 & 0 & 0 \\ 0 & 0 & 0 & 0 & G_5 & P_6 & 0 \\ 0 & 0 & 0 & 0 & 0 & G_6 & P_7 \end{bmatrix} \cdot \begin{bmatrix} ST_1 \\ ST_2 \\ ST_3 \\ ST_4 \\ ST_5 \\ ST_6 \\ ST_7 \end{bmatrix}_{t-1} \right)$$

$$+ \left(\begin{bmatrix} Pd_1 \\ 0 \\ 0 \\ 0 \\ 0 \\ 0 \\ 0 \end{bmatrix}_{t-1} \cdot \begin{bmatrix} ST_1 \\ ST_2 \\ ST_3 \\ ST_4 \\ ST_5 \\ ST_6 \\ ST_7 \end{bmatrix}_{t-1} \right)$$

where the Pd_1 vector is the probability of an organism rejecting the substrate, surviving, and entering the next time point as a pediveliger:

$$Pd_1 = S_1 \cdot [1 - (P_1 + G_1)] \quad (5)$$

The pulsed settlement regime describes a case in which all clams enter the model at the initial time point, whereas the diffused settlement regime has clams entering the model over a 10 d period following a Gaussian distribution. Additionally, pediveligers that did not settle at a given time point have the probability of surviving and entering the diffused pool at the next time point.

The *SR* 1 model, or the pulsed settlement regime, is specifically aimed at predicting the stage duration and growth to final stage class for all degrees of saturation state variability. The projection matrix model *SR* 2 (i.e. diffused settlement regime) simulates prolonged spawning events that occur in warmer waters (Eversole 2001 and references therein). Since diffused settlement is a specific life strategy for populations inhabiting warmer waters, we attempted to simulate this potentially beneficial process by examining the effect on cohort survival. It is important to note that no direct effect of temperature was applied to larval introduction or pediveliger settlement. Rather, this was a conceptual application to the model acknowledging the possibility of diffused spawning. The *SR* 2 model was, therefore, constructed to compare with the *SR* 1 model, as both were used to evaluate the interaction of temperature and saturation state variability given a population's biogeographical location and sea surface temperature. To determine any statistical and comparative differences, both the *SR 1* and *SR 2* projection matrix models were run at 1000 iterations for all 5 degrees of stochastic saturation state variability.

RESULTS

Model comparisons with field data

The maximum proportion of pediveligers settling and surviving to 35 d post-settlement in buffered and unbuffered sediments from the Green et al. (2013) study share a similar trend with our model simulations set at the same saturation states (Fig. 2). Comparison between our model projections and the Green et al. (2013) field data resulted in a root mean square error of 0.16 for the maximum proportion of juveniles counted in either the buffered or unbuffered scenarios. Model simulations underestimated the proportion of clams in undersaturated conditions (Ω_{ar} = 0.6) and overestimated those in supersaturated conditions (Ω_{ar} = 1.4). The model drastically underestimated the proportion of the maximum counted at ≤5 d; however, projection estimates improved at >10 d (Fig. 2).

Comparing stage duration at a constant saturation state

Stage duration for all post-larval juvenile size classes responded to both the saturation state and size of the organism (Fig. 4). Pediveligers were excluded because their stage duration follows the metric of settlement rather than calcification. Stage duration when growing in 0.2 mm increments ranged from ~2 d for 1.0 mm juveniles when Ω_{ar} ≥1.0, and ~15 d for 0.2 mm juveniles when Ω_{ar} was 0.2. Smaller juveniles took longer to transition to larger size classes across all saturation state values, and stage duration was reduced as saturation state and size-class increased. As conditions approached supersaturation (Ω_{ar} ≥1.0), the stage duration response to Ω_{ar} became negligible because the acidification effect is minimal on growth and survival when saturation state is ≥1.0; this response is based on previous experimental work (Green et al. 2004, 2009, Wald-

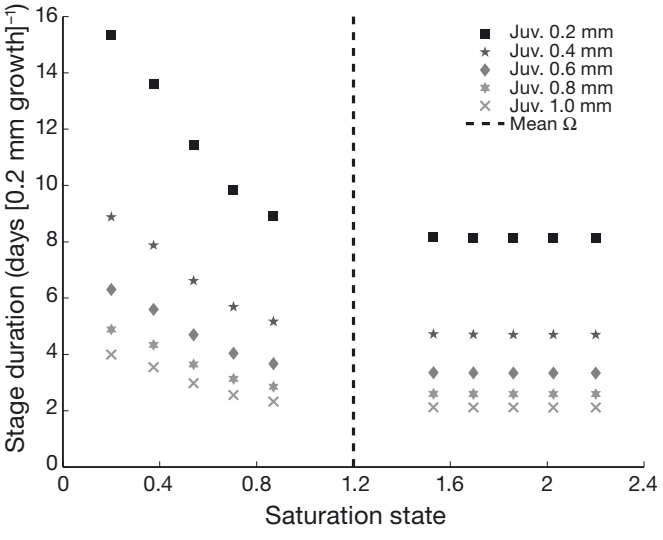

Fig. 4. Stage duration predicted by the model for juvenile size classes of hard clam *Mercenaria mercenaria* under different but constant (non-stochastic) saturation state scenarios. Discrete points are stage durations, shown as the number of days taken to achieve a 0.2 mm size increment, at the minimum and maximum Ω_{ar} values for each variability scenario (Fig. 3): low (central pair of Ω_{ar} values), low medium, medium, medium high, and high (extreme left and right Ω_{ar} values). Dashed black line shows the mean saturation state (Ω_{ar} = 1.2) for iterations run with stochastic variability

busser et al. 2010). We note that the discrete saturation state values for the stage duration analysis (Fig. 4) correspond to the minimum and maximum Ω_{ar} values of the variability scenarios used for other analyses, all of which share a common mean Ω_{ar} of 1.2 (dashed line in Fig. 4).

Acidification-dependent survival and growth

Survival rate and stage duration were adjusted on an hourly timescale according to the magnitude of each variability scenario (Fig. 2). Simulations run at the minimum saturation state values correspond to the lowest and highest variability scenarios, and resulted in a 182% difference in total survivors (n) at t_f (Fig. 5a), highlighting that periods below a saturation state of 1.0 have a greater effect on survivorship than periods above. The highest variability scenario induced the greatest magnitude of change in vital rates, which resulted in the lowest number of total survivors reaching the 2.0 mm 'escape size' stage class (Fig. 5b). Increasing saturation state variability from 33 to 100% of a full Ω_{ar} unit lengthened the number of days from 31 to 41, which corresponds to the time it took for 75% of surviving clams to reach the final 2.0 mm 'escape size' stage class (Fig. 5b). There was a ~60% difference in n between the lowest and highest variability scenarios, with the highest variability resulting in the lowest survival (Fig. 5b,c). Over 1000 iterations, the stochasticity applied to each variability scenario resulted in a 28% maximum difference between the number of survivors at any given iteration and the mean; however, the 95% CI for the mean number of survivors never exceed ±0.11 after the 1000 iterations.

Growth dynamics between temperature and saturation state

Compared to the constant mean saturation state of 1.2, each level of variability decreased n at t_f (Fig. 6). The total number of survivors under the constant mean saturation state scenario resulted in ~110 juvenile clams at t_f, whereas the total number of survivors at t_f for the high variability scenario was 55 juvenile clams. The 2:1 difference indicates that the effects of high saturation state variability exert a control on survivorship by reducing growth out of preceding, more sensitive, stage classes (Fig. 5b). In order for clams to increase survivorship and progress through the model at a rate that is analogous to the constant saturation state (Ω_{ar} = 1.2), intrinsic growth rates for each variability scenario would need to be very much higher as saturation state variability increased. Fig. 6 identifies the intrinsic growth rate needed for each variability scenario to match the total number of survivors under the constant saturation state scenario (with dashed bars and the rate in percent d^{-1}). For the high variability scenario, an intrinsic growth rate of 13.7% d^{-1} is needed to produce the same number of surviving juveniles in the final stage class at t_f as the constant saturation state scenario.

Increasing the intrinsic growth rate can mitigate the negative effects of saturation state variability on survivorship by accelerating transition out of the early, more sensitive stage classes (Fig. 6). Seawater temperature plays a functional role in cellular metabolism, and can increase growth rates if temperatures are optimal; the most favorable temperature in this respect is ~24°C (Ansell 1968, Hamwi & Haskin 1969). We identified 24°C as optimal, but recognize that sub-population growth rates may deviate ac-

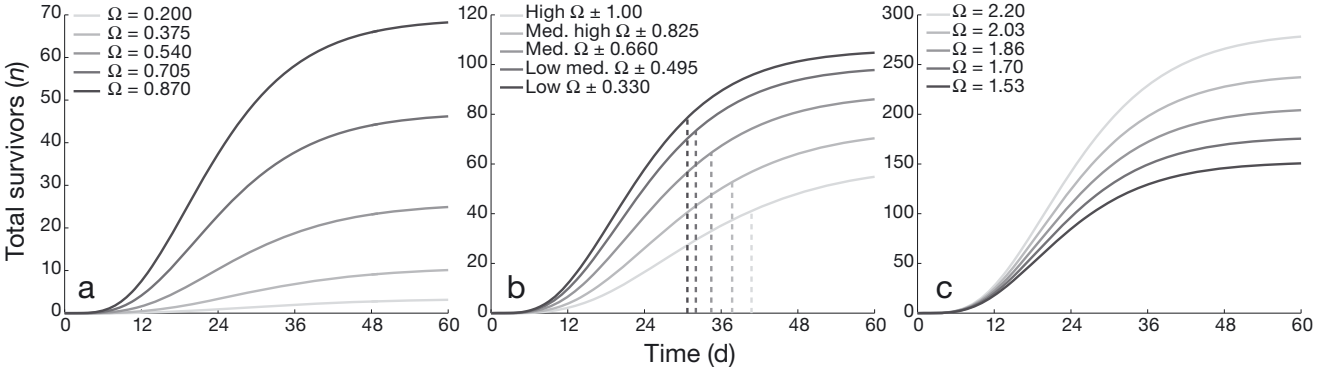

Fig. 5. Total number of survivors of hard clam *Mercenaria mercenaria* predicted by the model at (a) the minimum and (c) the maximum saturation states of each variability scenario: low (Ω_{ar} = 0.870 and 1.53), low medium, medium, medium high, and high (Ω_{ar} = 0.2 and 2.20). (b) Average values over 1000 simulations for each variability scenario with a mean omega value of 1.2; drop down dashed lines show the time in days that 75% of survivors reach the final stage class. The 95% CI for all variability scenarios was ≤0.164

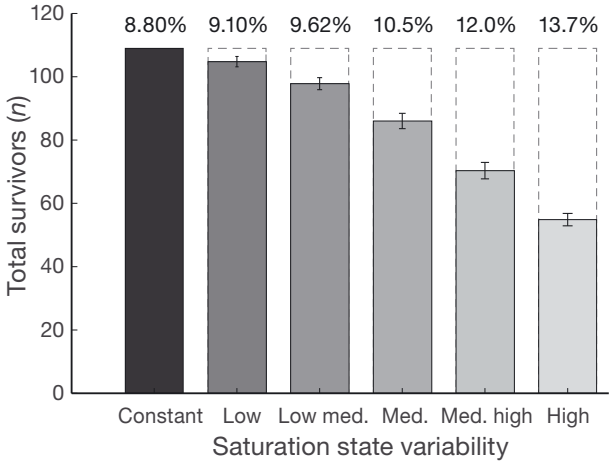

Fig. 6. Total number of survivors of hard clam *Mercenaria mercenaria* predicted by the model for the constant (mean) scenario (saturation state [Ω_{ar}] = 1.2) and each variability scenario (solid bars), with an intrinsic growth rate of 8.8% d^{-1} at an optimal 24°C. Dashed bars and percentages shown above them indicate the intrinsic growth rate needed for each variability scenario to equal the result of the mean (constant) saturation state. Error bars are the standard deviation of 1000 simulations

cording to habitat via other external factors (Grizzle et al. 2001). Table 2 shows the adjusted growth rate as a function of temperature and *Mercenaria mercenaria*'s thermal tolerance and optima. A spectrum of growth rates (Table 2) as a function of temperature was compared between the constant mean scenario as well as all variability scenarios (Fig. 7). Growth rate outside of the optimal range (17 and 27°C) had

Table 2. Intrinsic growth rates of hard clam *Mercenaria mercenaria* as a function of temperature. Average 2014 temperatures on North American east coast (44° 54.2′ to 28° 31.18′ N) for June and July (www.ndbc.noaa.gov) were used to calculate rates based on pediveliger response to temperature and optimum physiological temperature range (20–24°C) (Loosanoff 1959, Ansell 1968, Talmage & Gobler 2011)

Temperature (°C)	Intrinsic growth (% d^{-1})
17	6.7
20	7.5
22	8.2
24	8.8
27	7.1

the lowest percent survivors at t_f for all variability scenarios. Under higher saturation state variability, the difference in percent survivors across different temperatures decreased (Fig 7a). That is, a smaller difference was observed between the high variability scenarios for all temperature-dependent growth rates simulated. The temperature growth rate simulations were run using the *SR* 1 (Fig. 7a) and *SR* 2 (Fig. 7b) models. Both model simulations produced the same trends and resulted in little difference between the percent survivors. The greatest difference in percent survivors between the 2 model simulations was only 6.7% at t_f, and this was at a growth rate of 17°C with high saturation state variability (Fig. 7). All significant differences (i.e. non-overlapping error bars), therefore, are a result of growth rate differences and not the model used for simulations.

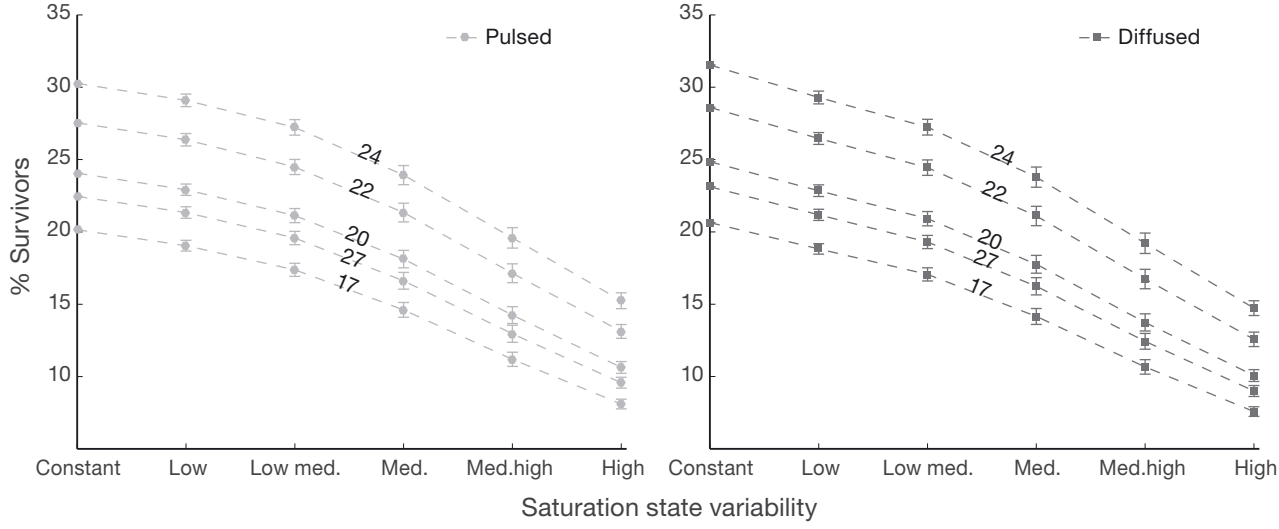

Fig. 7. Average percent survivors of hard clam *Mercenaria mercenaria* predicted from 1000 model simulations to reach 'escape size' (2.0 mm) at the final time point for the constant (mean) scenario (saturation state [Ω_{ar}] = 1.2) and each variability scenario. Simulations were run under (a) pulsed and (b) diffuse settlement regimes. Contour lines represent a constant temperature (°C) that corresponds to an associated intrinsic growth rate (Table 2). Error bars are the standard deviation of 1000 simulations

DISCUSSION

The developmental period of newly settled post-larval bivalves is a vulnerable and critical period, where survivorship and successful transition to more developed stages can determine the dynamics and recruitment of adult bivalves (Roegner & Mann 1995, Gosselin & Qian 1997). We utilized the results of the limited studies that documented the effects of acidification on the early developmental stages of post-larval *Mercenaria mercenaria* (Green et al. 2009, 2013, Waldbusser et al. 2010) to predict acidification sensitivity during this important transition. According to our model, the magnitude of acidification has a large effect on the settlement of larval clams, and on the stage duration of post-larval development. In addition, projections illustrate scenarios in which increases in temperature could accelerate transition through early, more sensitive stage classes. Our model elucidates one way the effects of acidification can impact the success of a cohort, and could be used to corroborate comprehensive population models that examine the physiological development associated with genetic variance in ecotypes, feeding rates, and variations in temperature and salinity (Hofmann et al. 2006). By examining the effects of acidification on specific post-metamorphic developmental stages, we can simulate how progression of OA and increasingly episodic eutrophication events may affect *M. mercenaria* cohort success through this critical life-history bottleneck. While our model does not consider the effects of post-settlement advection, short-term acclimatization, carry-over effects, or predation —which can increase with warmer temperatures (Beal et al. 2001)— we have moderate confidence in the model dynamics given the general coherence between the model and field data (Fig. 2) from Green et al. (2013).

When compared to the Green et al. (2013) field data, our model heavily underestimates the proportion of the maximum counted at ≤5 d (Fig. 2). This is due to the fact that the Green et al. (2013) study counted all clams regardless of size, whereas our model estimates of maximum proportion counted relied on clams reaching the final stage; therefore, predictions did not show abundances in the first few days. Small-scale spatial heterogeneity in sediment saturation state, and the continued settlement of clams over the duration of the field experiment may be reasons why model projections underestimated proportion of the maximum in unbuffered sediments. The overestimated projection for the control sediment patch is likely due to other modes of mortality, such as predation. While our model does not exactly match the field data of *Mya arenaria,* which may respond differently than *M. mercenaria*, the general response to OA is striking. In addition, our model is not inclusive of developmental stages occurring before the pediveliger stage, where sensitivities are present and manifest as delayed growth and abnormal development, which can carry-over into juvenile stages (Talmage & Gobler 2010, Barton et al. 2012, Hettinger et al. 2012). The potential for short-term acclimatization is also not captured here, as shifts in metabolic energy can change physiological mechanisms and biochemical pathways that adjust to maintain homeostasis when exposed to environmental stressors (Applebaum et al. 2014, Pan et al. 2015). Future model iterations could include an ancillary model that independently parameterizes saturation state (e.g. organic matter respiration rate), and incorporates other sediment biogeochemical processes, such as the effects of calcification (resulting in net reduction of alkalinity) and dissolution, as well as macroinfauna effects on biogeochemical exchanges (e.g. flux of NH_4^+ and H_2S, both of which are negative recruitment cues) (Krumins et al. 2013).

Acidification disproportionality affects the stage-duration of smaller juveniles compared to larger juveniles (Fig. 4) by reducing calcification rates (growth), inhibiting organogenesis, or by delaying metamorphosis and settlement (Talmage & Gobler 2009, Waldbusser et al. 2010, Green et al. 2013). Successful development and escape to more resilient life-stages then becomes a function of how quickly post-larval clams can transition through the more sensitive stages where energy acquisition is limited due to low feeding rates and underdeveloped siphons (Bayne & Newell 1983). The parameterization of our model captures this interaction between growth and size when under acidification (Fig. 4). The ability to grow and transition to larger stage classes while resisting internal shell corrosion and maintaining homeostasis under acidification has been shown to be coupled to internal energy budgets and the ability to efficiently acquire food in older juvenile mussels, >10 mm shell length (Melzner et al. 2011). In addition, Waldbusser et al. (2013, 2015) found that larval bivalves 48 h post-fertilization respond most first to saturation state, and proposed that the rate of calcification for the initial shell layer is dependent on saturation state, with the relationship expressed as a kinetic-energetic constraint. Whether or not rapid biocalcification is relevant during metamorphosis, there are developmental similarities between the production of the first shell layer and

metamorphosis, such that organogenesis, shell growth, and homeostasis are dependent on internal energy budgets during non-feeding periods, which require higher than normal amounts of energy when under the effects of acidification. Once feeding appendages develop, high rates of energy intake are most likely needed to help compensate for the large energetic demand of organogenesis, and to resist acidification stress through acid–base regulation via active ion transport across membranes, internal HCO_3^- buffering, or by controlling respiration (Walsh & Milligan 1989, García-Esquivel et al. 2001, Waldbusser et al. 2013).

Periods of favorable carbonate chemistry can occur temporally when systems become net autotrophic during daylight hours (Barranguet et al. 1998, Tang & Kristensen 2007, Glud 2008, Fischer & Wenzhofer 2010), potentially mitigating the effects of acidification on hourly timescales. Given the short time period in which settlement, metamorphosis, and post-metamorphosis growth occur (Carriker 2001 and references therein), the dynamic range of carbonate chemistry diurnal variability is likely a significant component determining *M. mercenaria* survivorship response to the effects of acidification, and delineates the importance of settlement timing and metamorphosis to periods when carbonate chemistry is more favorable. Previous studies have highlighted the extreme variability of the carbonate system in near-shore coastal waters, and describe the uncertainty of how biological systems will respond to future CO_2 intrusion and eutrophication (Andersson et al. 2006, Feely et al. 2008, 2010, Harris et al. 2013). By modulating saturation state over a diurnal period, we attempted to capture the effect of acidification severity (the integrated duration and intensity), illustrating how post-larval clam stage duration and survival rate respond to acute acidification (Table 3, Fig. 5). It should be noted that our model does not allow for compensatory growth (i.e. an accelerated growth rate following a period of growth or development), if that occurs on timescales of several hours. The high variability scenario, therefore, extended the magnitude of exposure to unfavorable and favorable conditions, which resulted in a stage duration ~10 d longer from the lowest variability scenario, and reduced the total number of juveniles reaching 'escape-size' (Fig. 5b). Given that all of our variability scenarios share a common mean (i.e. equal hourly duration when Ω_{ar} <1.0), the differences between our simulations are a result of the magnitude of acidification, which affects the severity (Table 3). Severity seems to accurately represent our findings because calcifying organismal health correlates to the short-term integrated effects of acidification (Beesley et al. 2008, Wood et al. 2008), which fluctuates naturally in coastal shallow-water deposits (Green & Aller 1998). Small et al. (2015a) recently pointed out that the acute stress on acid–base regulation under naturally high pCO_2 variability may determine future winners and losers via the mechanisms in which calcifying organisms regulate their acid-base equilibrium. While there is some evidence to suggest that hourly shifts in carbonic anhydrase production may be a response to acidosis (Connor & Gracey 2011), other studies identify longer timescales for acid–base regulation (Pane & Barry 2007, Melzner et al. 2009). The timescale differences in response, however, are critical given that the duration and magnitude at which acidosis occurs will determine the energetic investment that must be put into maintaining acid-base homeostasis. That is, regardless of the species-specific mechanism of acid-base regulation, there must be sufficient amounts of metabolic energy that can be invested to carry out these regulating processes, and metamorphosis is an energetically demanding stage in itself.

Based on our model projections, increasing intrinsic growth rate would be a key mechanism by which *M. mercenaria* could reduce the stage duration of sensitive post-larval stages, and thus increase overall survival. We manipulated intrinsic growth rate for all variability scenarios to determine the minimum growth rate needed to equal the number of total survivors under the constant mean scenario (Fig. 6). Our model suggests post-larval clams would need to in-

Table 3. Variability scenarios used to model life stage development of hard clam *Mercenaria mercenaria,* showing effects of saturation state (Ω) variability around a mean/threshold value of 1.2. Ω_{UTR} is the under threshold range that persists for 11 h over a 24 h period, represented as 1 × 11 array. Intensity is the difference between the 1.2 saturation state threshold/mean and the average saturation state values from 1000 iterations that are under the threshold value (Ω_{UV}) in a diurnal period (e.g. intensity value = 1.2–1.0) (Sheffield & Wood 2008, Hauri et al. 2013). All intensity values were integrated for the entire duration: 11 h

Variability		Ω_{mean}	Ω_{UTR}	Duration	Intensity	Severity
Scenario	Magnitude			(h)	(Ω_{mean} – Ω_{UV})	I × D
Low	±0.33	1.2	0.05 – 0.33	11	2.3	25
Low medium	±0.495	1.2	0.09 – 0.49	11	3.5	38
Medium	±0.66	1.2	0.11 –0.65	11	4.6	51
Medium high	±0.825	1.2	0.14 – 0.82	11	5.8	63
High	±1.0	1.2	0.18 – 0.99	11	7	77

crease calcification by a minimum of 3.0% and up to 56% for a highly variable aragonite saturation state. Increasing calcification by 56% may be possible in some individuals considering the high variance in growth rates just within a single cohort; however, the inherent factors determining growth variance are difficult to tease apart, and high growth rates are not consistent enough among *M. mercenaria* larvae to positively affect a significant proportion of a cohort (Przeslawski & Webb 2009). We would be remiss if we did note not that we are unaware of studies that would indicate what degree of compensatory growth is possible at these early life stages, which could be one mechanism by which our modeled effects could be mitigated. Hybridization between *Mercenaria* species (*M. mercenaria* × *M. campechiensis*) has also been shown to produce growth rates that are more than double that of *M. mercenaria,* and could explain the significant differences found in calcification rate between 2 geographically separated cohorts (Arnold et al. 1996, 1998, Waldbusser et al. 2010). The genetic variability acting upon *M. mercenaria* growth rate is complex, and shifts throughout ontogentic development, as well as across habitats, making selective breeding for *M. mercenaria* growth enhancement difficult and inconclusive (Hilbish et al. 1993, Arnold et al. 1998, Grizzle et al. 2001, Hilbish 2001). While it remains unclear whether or not differences in genotypic growth traits exist throughout *M. mercenaria*'s latitudinal distribution (Hilbish 2001), it is suggested that the genetic variation throughout *M. mercenaria* populations is homogenous, indicating that genotypic enhanced growth can occur for any geographical population (Rawson & Hilbish 1991, Hilbish 2001).

The most significant environmental factor that affects growth rate is temperature (Grizzle et al. 2001 and references therein). While food quality and quantity is also a significant factor determining growth, and at the right combinations can elicit a 4-fold increase in growth rate (Walne 1970, Bayne & Newell 1983, MacDonald et al. 1998), temperature is still found to be the major environmental determinate (Grizzle et al. 2001 and references therein, Weiss et al. 2007). The biogeographical range of *M. mercenaria* populations extends across a latitudinal gradient of sea surface temperatures that directly affect clam growth rates, with annual measurements of shell length found to be consistently higher for southern populations despite large seasonal variations in growth rate, with maximum growth rates occurring between 20 and 24°C (Ansell 1968, Grizzle et al. 2001 and references therein). Even though most studies have only examined annual temperature-dependent growth rates, there is evidence to suggest that the annual rates correlate to shorter timescales and acute responses (Loosanoff 1959, Weiss et al. 2007, Talmage & Gobler 2011), as does the temperature optima determined from annual growth rates (Hamwi & Haskin 1969). We therefore, incorporated temperature-dependent growth rates (Table 2) to determine changes in total percent survivors (Fig. 7). We ran these simulations under both the pulsed and diffused models, and found the percent difference in survivors to be trivial (≤6.7%). This suggests that our model may not have efficiently captured the diffused spawning life strategy, which could potentially improve cohort success. This may be due to the fact that model simulations only ran for 60 d. Therefore, it is possible that a portion of individuals never reached the 2.0 mm stage class if they entered the model 5–10 d after it began, which would reduce the total number of survivors at t_f. The overall significant differences in total percent survivors were, then, due to the differences in growth rate and not diffused introduction (Fig. 7), highlighting that rapid progression through sensitive life-history stages may be a critical strategy and trait for post-larval clams to cope with OA.

The highly variable nature of coastal ocean carbonate chemistry represents a challenging setting, in which our model attempts to predict how late larval and post-larval *M. mercenaria* will respond under various future climate change scenarios. With myriad factors determining survivorship and adult recruitment (Gosselin & Qian 1997, Fegley 2001, Green et al. 2009), the negative effects of acidification may be a growing contributor to *M. mercenaria* cohort success in wild populations. Coincidently, however, increasing sea surface temperatures may prove to be a mitigating factor from the deleterious effects of acidification, with evidence showing that temperature increase within an organism's thermal tolerance can offset the effects of acidification on growth, development, and settlement (Waldbusser et al. 2011, Kroeker et al. 2014, García et al. 2015). This finding should be considered carefully, however, as other studies have found that temperature increases beyond thermal thresholds interact synergistically with increased pCO_2 to lower physiological tolerance to high CO_2 concentrations (Pörtner 2008, Talmage & Gobler 2011). Further investigation is needed to corroborate our model findings of the positive effect temperature may have on specific ecotypes of *M. mercenaria*, particularly when these potential multi-stressors create mosaics of complex environmental and biological interactions that affect an organism's performance

during specific developmental stages for marine calcifiers (Small et al. 2015b, Kroeker et al. 2016). Our model exploring the effects of acidification on a post-larval *M. mercenaria* cohort is an initial step toward a better understanding of how growth and acidification sensitivity during this critical life-stage can predict future 'winners' and 'losers' in a warming and high-CO_2 world. Further, our model provides a basis for predicting biological responses in the context of acidification severity, which better captures the natural responses of biological systems to variable carbonate chemistry (Hauri et al. 2013), and has the potential to be incorporated into future biophysical monitoring efforts that are aimed at supporting the local community structure and economic stability of shellfish aquaculture.

Acknowledgements. This work was supported by the Increasing Diversity in Earth Sciences research internship program at Oregon State University. Funding for the research internship was granted to the program coordinators and recipients of National Science Foundation EAR #0914707: Shanaka de Silva, Lynette de Silva, and Robert Duncan. The authors thank Drs. M. A. Green and S. E. Kolesar for the conceptual assistance for early model iterations, and the 3 anonymous reviewers for critical feedback that has improved this manuscript.

LITERATURE CITED

Aller R (1982) Carbonate Dissolution in nearshore terrigenous muds: the role of physical and biological reworking. J Geol 90:79–95

Andersson AJ, Mackenzie FT, Lerman A (2006) Coastal ocean CO_2-carbonic acid-carbonate sediment system of the anthropocene. Global Biogeochem Cycles 20: GB1S92

Ansell AD (1968) The rate of growth of the hard clam *Mercenaria mercenaria* (L) throughout the geographical range. J Cons Int Explor Mer 31:364–409

Applebaum SL, Pan TCF, Hedgecock D, Manahan DT (2014) Separating the nature and nurture of the allocation of energy in response to global change. Integr Comp Biol 54:284–295

Arnold WS, Bert TM, Marelli DC, Cruz Lopez H, Gill PA (1996) Genotype specific growth of hard clams (genus *Mercenaria*) in a hybrid zone: variation among habitats. Mar Biol 125:129–139

Arnold WS, Bert TM, Quitmyer IR, Jones DS (1998) Contemporaneous deposition of annual growth bands in *Mercenaria mercenaria* (Linnaeus), *Mercenaria campechiensis* (Gmelin), and their natural hybrid forms. J Exp Mar Biol Ecol 223:93–109

Barranguet C, Kromkamp J, Peene J (1998) Factors controlling primary production and photosynthetic characteristics of intertidal microphytobenthos. Mar Ecol Prog Ser 173:117–126

Barton A, Hales B, Waldbusser GG, Langdon C, Feely RA (2012) The Pacific oyster, *Crassostrea gigas*, shows negative correlation to naturally elevated carbon dioxide levels: implications for near-term ocean acidification effects. Limnol Oceanogr 57:698–710

Bayne BL, Newell RC (1983) Physiological energetics of marine molluscs. In: Saleuddin ASM, Wilber KM (eds) The Mollusca, Vol. 4: physiology, Part 1. Academic Press, New York, NY, p 407–515

Beal BF, Parker MR, Vencile KW (2001) Seasonal effects of intraspecific density and predator exclusion along a shore-level gradient on survival and growth of juveniles of the soft-shell clam, *Mya arenaria* L., in Maine, USA. J Exp Mar Biol Ecol 264:133–169

Beesley A, Lowe DM, Pascoe CK, Widdicombe S (2008) Effects of CO_2-induced seawater acidification on the health of *Mytilus edulis*. Clim Res 37:215–225

Caldeira K, Wickett ME (2003) Anthropogenic carbon and ocean pH. Nature 425:365

Carriker MR (1961) Interrelation of functional morphology, behavior, and autecology in early stages of the bivalve *Mercenaria mercenaria*. J Elisha Mitchell Sci Soc 77: 168–241

Carriker MR (2001) Embryogenesis and organogenesis of veligers and early juveniles. In: Kraeuter JN, Castagna M (eds) Biology of the hard clam. Elsevier, Amsterdam, p 77–115

Connor KM, Gracey AY (2011) Circadian cycles are the dominant transcriptional rhythm in the intertidal mussel *Mytilus californianus*. Proc Natl Acad Sci USA 108: 16110–16115

Crouse D, Crowder L, Caswell H (1987) A stage-based population model for loggerhead sea turtles and implications for conservation. Ecology 68:1412–1423

Doney SC, Fabry VJ, Feely RA, Kleypas JA (2009) Ocean acidification: the other CO_2 problem. Annu Rev Mar Sci 1:169–192

Eversole AG (2001) Reproduction in *Mercenaria mercenaria*. In: Kraeuter JN, Castagna M (eds) Biology of the hard clam. Elsevier, Amsterdam, p 221–260

Feely RA, Sabine CL, Lee K, Berelson W, Kleypas J, Fabry VJ, Millero FJ (2004) Impact of anthropogenic CO_2 on the $CaCO_3$ system in the oceans. Science 305:362–366

Feely RA, Sabine CL, Hernandez-Ayon JM, Ianson D, Hales B (2008) Evidence for upwelling of corrosive 'acidified' water onto the continental shelf. Science 320: 1490–1492

Feely RA, Alin SR, Newton J, Sabine CL and others (2010) The combined effects of ocean acidification, mixing, and respiration on pH and carbonate saturation in an urbanized estuary. Estuar Coast Shelf Sci 88:442–449

Fegley SR (2001) Demography and dynamics of hard clam populations. In: Kraeuter JN, Castagna M (eds) Biology of the hard clam. Elsevier, Amsterdam, p 383–422

Fischer JP, Wenzhofer F (2010) A novel planar optode setup for concurrent oxygen and light field imaging: application to a benthic phototrophic community. Limnol Oceanogr Methods 8:254–268

García E, Clemente S, Hernández JC (2015) Ocean warming ameliorates the negative effects of ocean acidification on *Paracentrotus lividus* larval development and settlement. Mar Environ Res 110:61–68

García-Esquivel Z, Bricelj VM, Gonzalez-Gomez MA (2001) Physiological basis for energy demands and early post-larval mortality in the Pacific oyster, *Crassostrea gigas*. J Exp Mar Biol Ecol 263:77–103

Glud RN (2008) Oxygen dynamics of marine sediments. Mar Biol Res 4:243–289

Gosselin LA, Qian PY (1997) Juvenile mortality in benthic marine invertebrates. Mar Ecol Prog Ser 146:265–282

Green MA, Aller RC (1998) Seasonal patterns of carbonate diagenesis in nearshore terrigenous muds: relation to spring phytoplankton bloom and temperature. J Mar Res 56:1097–1123

Green MA, Aller RC (2001) Early diagenesis of calcium carbonate in Long Island Sound sediments: benthic fluxes of Ca^{2+} and minor elements during seasonal periods of net dissolution. J Mar Res 59:769–794

Green MA, Jones ME, Boudreau CL, Moore RL, Westman BA (2004) Dissolution mortality of juvenile bivalves in coastal marine deposits. Limnol Oceanogr 49:727–734

Green MA, Waldbusser GG, Reilly SL, Emerson K, O'Donnell S (2009) Death by dissolution: sediment saturation state as a mortality factor for juvenile bivalves. Limnol Oceanogr 54:1037–1047

Green MA, Waldbusser GG, Hubazc L, Cathcart E, Hall J (2013) Carbonate mineral saturation state as the recruitment cue for settling bivalves in marine muds. Estuaries Coasts 36:18–27

Grizzle RE, Bricelj VM, Shumway SE (2001) Physiological ecology of *Mercenaria mercenaria*. In: Kraeuter JN, Castagna M (eds) Biology of the hard clam. Elsevier, Amsterdam, p 305–382

Hales B, Suhrbier A, Waldbusser GG, Feely RA, Newton J (2016) The carbonate chemistry of the 'fattening line,' Willapa Bay, 2011–2014. Estuar Coasts doi: 10/1007/s12237-016-0136-7

Hamwi A, Haskin HH (1969) Oxygen consumption and pumping rates in the hard clam *Mercenaria mercenaria*: a direct method. Science 163:823–824

Harris KE, DeGrandpre MD, Hales B (2013) Aragonite saturation state dynamics in a coastal upwelling zone. Geophys Res Lett 40:2720–2725

Hauri C, Gruber N, McDonnell AMP, Vogt M (2013) The intensity, duration, and severity of low aragonite saturation state events on the California continental shelf. Geophys Res Lett 40:3424–3428

Hettinger A, Sanford E, Hill TM, Russell AD and others (2012) Persistent carry-over effects of planktonic exposure to ocean acidification in the Olympia oyster. Ecology 93:2758–2768

Hilbish TJ (2001) Genetics of hard clams, *Mercenaria mercenaria*. In: Kraeuter JN, Castagna M (eds) Biology of the hard clam. Elsevier, Amsterdam, p 261–280

Hilbish T, Winn E, Rawson P (1993) Genetic variation and covariation during larval and juvenile growth in *Mercenaria mercenaria.* Mar Biol 115:97–104

Hofmann EE, Klinck JM, Kraeuter JN, Powell EN, Grizzle RE, Buckner SC, Bricelj VM (2006) Population dynamics model of the hard clam, *Mercenaria mercenaria*: development of the age- and length-frequency structure of the population. J Shellfish Res 25:417–444

Hönisch B, Ridgwell A, Schmidt DN, Thomas E and others (2012) The geological record of ocean acidification. Science 335:1058–1063

Hunt HL, Scheibling RE (1997) Role of early post-settlement mortality in recruitment of benthic marine invertebrates. Mar Ecol Prog Ser 155:269–301

Kroeker KJ, Gaylord B, Hill TM, Hosfelt JD, Miller SH, Sanford E (2014) The Role of temperature in determining species' vulnerability to ocean acidification: a case study using *Mytilus galloprovincialis.* PLOS ONE 9: e100353

Kroeker KJ, Sanford E, Rose JM, Blanchette CA and others (2016) Interacting environmental mosaics drive geographic variation in mussel performance and predation vulnerability. Ecol Lett 19:771–779

Krumins V, Gehlen M, Arndt S, Van Cappellen P, Regnier P (2013) Dissolved inorganic carbon and alkalinity fluxes from coastal marine sediments: model estimates for different shelf environments and sensitivity to global change. Biogeosciences 10:371–398

Lefkovitch LP (1965) The study of population growth in organisms grouped by stages. Biometrics 21:1–18

Loosanoff VL (1959) The size and shape of metamorphosing larvae of *Venus* (*Mercenaria*) *mercenaria* grown at different temperatures. Biol Bull 117:308–318

Lowenstam HA (1981) Minerals formed by organisms. Science 211:1126–1131

MacDonald BA, Bacon GS, Ward JE (1998) Physiological responses of infaunal (*Mya arenaria*) and epifaunal (*Placopecten magellanicus*) bivalves to variations in the concentration and quality of suspended particles: II. Absorption efficiency and scope for growth. J Exp Mar Biol Ecol 219:127–141

McConnaughey TA, Gillikin DP (2008) Carbon isotopes in mollusk shell carbonates. Geo-Mar Lett 28:287–299

Melzner F, Gutowska MA, Langenbuch M, Dupont S and others (2009) Physiological basis for high CO_2 tolerance in marine ectothermic animals: pre-adaptation through lifestyle and ontogeny? Biogeosciences 6:2313–2331

Melzner F, Stange P, Truebenbach K, Thomsen J and others (2011) Food supply and seawater pCO_2 impact calcification and internal shell dissolution in the blue mussel *Mytilus edulis*. PLOS ONE 6:e24223

Ólafsson E, Peterson C, Ambrose W (1994) Does recruitment limitation structure populations and communities of macroinvertebrates in marine soft sediments: the relative significance of pre- and post-settlement processes. Oceanogr Mar Biol Annu Rev 32:65–109

Orr JC, Fabry VJ, Aumont O, Bopp L and others (2005) Anthropogenic ocean acidification over the twenty-first century and its impact on calcifying organisms. Nature 437:681–686

Palmer AR (1992) Calcification in marine mollusks: how costly is it? Proc Natl Acad Sci USA 89:1379–1382

Pan TCF, Applebaum SL, Manahan DT (2015) Experimental ocean acidification alters the allocation of metabolic energy. Proc Natl Acad Sci USA 112:4696–4701

Pane EF, Barry JP (2007) Extracellular acid–base regulation during short-term hypercapnia is effective in a shallow-water crab, but ineffective in a deep-sea crab. Mar Ecol Prog Ser 334:1–9

Pörtner HO (2008) Ecosystem effects of ocean acidification in times of ocean warming: a physiologist's view. Mar Ecol Prog Ser 373:203–217

Przeslawski R, Webb AR (2009) Natural variation in larval size and developmental rate of the northern quahog *Mercenaria mercenaria* and associated effects on larval and juvenile fitness. J Shellfish Res 28:505–510

Queirós AM, Taylor P, Cowles A, Reynolds A, Widdicombe S, Stahl H (2015) Optical assessment of impact and recovery of sedimentary pH profiles in ocean acidification and carbon capture and storage research. Int J Greenh Gas Control 38:110–120

Rawson P, Hilbish T (1991) Genotype-environment interaction for juvenile growth in the hard clam *Mercenaria mercenaria* (L.). Evolution 45:1924–1935

Roegner GC, Mann R (1995) Early recruitment and growth of the American oyster *Crassostrea virginica* (Bivalvia: Ostreidae) with respect to tidal zonation and season. Mar Ecol Prog Ser 117:91–101

Sheffield J, Wood EF (2008) Projected changes in drought occurrence under future global warming from multi-model, multi-scenario, IPCC AR4 simulations. Clim Dyn 31:79–105

Small DP, Calosi P, Boothroyd D, Widdicombe S, Spicer JI (2015a) Stage-specific changes in physiological and life-history responses to elevated temperature and pCO_2 during the larval development of the European lobster *Homarus gammarus* (L.). Physiol Biochem Zool 88: 494–507

Small DP, Milazzo M, Bertolini C, Graham H, Hauton C, Hall-Spencer JM, Rastrick SPS (2015b) Temporal fluctuations in seawater pCO_2 may be as important as mean differences when determining physiological sensitivity in natural systems. ICES J Mar Sci 73:604–612

Talmage SC, Gobler CJ (2009) The effects of elevated carbon dioxide concentrations on the metamorphosis, size, and survival of larval hard clams (*Mercenaria mercenaria*), bay scallops (*Argopecten irradians*), and eastern oysters (*Crassostrea virginica*). Limnol Oceanogr 54:2072–2080

Talmage SC, Gobler CJ (2010) Effects of past, present, and future ocean carbon dioxide concentrations on the growth and survival of larval shellfish. Proc Natl Acad Sci USA 107:17246–17251

Talmage SC, Gobler CJ (2011) Effects of elevated temperature and carbon dioxide on the growth and survival of larvae and juveniles of three species of northwest Atlantic bivalves. PLOS ONE 6:e26941

Tang M, Kristensen E (2007) Impact of microphytobenthos and macroinfauna on temporal variation of benthic metabolism in shallow coastal sediments. J Exp Mar Biol Ecol 349:99–112

Thomsen J, Haynert K, Wegner KM, Melzner F (2015) Impact of seawater carbonate chemistry on the calcification of marine bivalves. Biogeosciences 12:4209–4220

Thorson G (1966) Some factors influencing the recruitment and establishment of marine benthic communities. Neth J Sea Res 3:267–293

Waldbusser GG, Salisbury JE (2014) Ocean acidification in the coastal zone from an organism's perspective: multiple system parameters, frequency domains, and habitats. Annu Rev Mar Sci 6:221–247

Waldbusser GG, Bergschneider H, Green MA (2010) Size-dependent pH effect on calcification in post-larval hard clam *Mercenaria* spp. Mar Ecol Prog Ser 417:171–182

Waldbusser GG, Voigt EP, Bergschneider H, Green MA, Newell RIE (2011) Biocalcification in the eastern oyster (*Crassostrea virginica*) in relation to long-term trends in Chesapeake Bay pH. Estuaries Coasts 34:221–231

Waldbusser GG, Brunner EL, Haley BA, Hales B, Langdon CJ, Prahl FG (2013) A developmental and energetic basis linking larval oyster shell formation to acidification sensitivity. Geophys Res Lett 40:2171–2176

Waldbusser GG, Hales B, Langdon CJ, Haley BA and others (2015) Saturation-state sensitivity of marine bivalve larvae to ocean acidification. Nat Clim Change 5:273–280

Waldbusser GG, Hales B, Haley BA (2016) Calcium carbonate saturation state: on myths and this or that stories. ICES J Mar Sci 73:563–568

Walne PR (1970) Studies on the food value of nineteen genera of algae to juvenile bivalves of the genera *Ostrea*, *Crassostrea*, *Mercenaria* and *Mytilus*. Fishery Investigations, Series II 26:1–62

Walsh P, Milligan C (1989) Coordination of metabolism and intracellular acid-base status: ionic regulation and metabolic consequences. Can J Zool 67:2994–3004

Weiss MB, Curran PB, Peterson BJ, Gobler CJ (2007) The influence of plankton composition and water quality on hard clam (*Mercenaria mercenaria* L.) populations across Long Island's south shore lagoon estuaries (New York, USA). J Exp Mar Biol Ecol 345:12–25

Wenzhofer F, Glud RN (2004) Small-scale spatial and temporal variability in coastal benthic O_2 dynamics: effects of fauna activity. Limnol Oceanogr 49:1471–1481

Wood HL, Spicer JI, Widdicombe S (2008) Ocean acidification may increase calcification rates, but at a cost. Proc R Soc B 275:1767–1773

Zwarts L, Wanink J (1989) Siphon size and burying depth in deposit-feeding and suspension-feeding benthic bivalves. Mar Biol 100:227–240

Editorial responsibility: Romuald Lipcius, Gloucester Point, Virginia, USA

Submitted: January 28, 2016; Accepted: August 28, 2016
Proofs received from author(s): October 4, 2016